arXiv:1602.02257v1 [cond-mat.stat-mech] 6 Feb 2016

The Anisotropic Four-State Clock Model in the Presence of Random Fields

Octavio D. Rodriguez Salmon*

Departamento de Física

Universidade Federal do Amazonas, 3000, Japiim

69077-000 Manaus - AM Brazil

Fernando D. Nobre†

Centro Brasileiro de Pesquisas Físicas and

National Institute of Science and Technology for Complex Systems

Rua Xavier Sigaud 150

22290-180 Rio de Janeiro - RJ Brazil

(Dated: February 9, 2016)

A four-state clock ferromagnetic model is studied in the presence of different configurations of anisotropies and random fields. The model is considered in the limit of infinite-range interactions, for which the mean-field approach becomes exact. Both representations of Cartesian spin components and two Ising variables are used, in terms of which the physical properties and phase diagrams are discussed. The random fields follow bimodal probability distributions and the richest criticality is found when the fields, applied in the two Ising systems, are not correlated. The phase diagrams present new interesting topologies, with a wide variety of critical points, which are expected to be useful in describing different complex phenomena.

Keywords: Multicritical Phenomena, Random-Field Ising Model, Plastic Crystals.

PACS numbers: 05.70.Fh, 05.70.Jk, 64.60.-i, 64.60.Kw, 75.10.Hk

*E-mail address:octaviors@gmail.com

†Corresponding author: E-mail address: fdnobre@cbpf.br

I. INTRODUCTION

Spin models represent the most successful applications of statistical mechanics and have played an important role in the development of this theory [1, 2]. Among those, the Ising model is by far the most investigated, being able to describe satisfactorily many magnetic materials [3]. Apart form this, variations of Ising model have been considered also for modeling a wide variety of systems outside of magnetism, like metallic alloys, lattice gases, biological, social, and financial systems.

The introduction of disorder in the Ising model, either in the spin-spin interactions (e.g., interactions following a symmetric probability distribution, resulting in the Ising spin-glass model), and/or by means of a random field acting on each spin variable (defining the random-field Ising model), has led to further physical realizations, open problems, and controversial aspects [4–6]. At the infinite-range interaction limit, for which the mean-field approach becomes exact, these models have exhibited curious properties, and in some cases, very rich critical phenomena that has attracted the attention of many researchers [7–24]). Even though some properties and criticality found at the mean-field level may not occur in more realistic models, defined in terms of short-range interactions, random Ising models have been useful for investigating several systems, out of the scope of magnetism, like neural networks, proteins (particularly, in the study of protein folding), optimization problems, and plastic crystals.

The plastic crystals are compounds that present an intermediate stable state (called plastic phase) between a high-temperature (disordered) liquid phase, and a low-temperature (ordered) solid phase. In such intermediate state, rotational disorder coexists with translational order, characterized by the centers of mass of the molecules forming a regular crystalline lattice, with the molecules presenting disorder in their orientational degrees of freedom. These systems were treated in the literature by means of two sets of Ising spin variables representing, respectively, the orientational and translational degrees of freedom, in addition to a random field acting on one set of variables [15, 22–25].

Other spin models, mostly defined as generalizations of the Ising model, have been much studied in the literature [26]; among those, one should mention the p-state Potts model [27], which appears very often in situations where discrete variables with more than two states are required for an appropriate description of a given system. As examples

of realizations, one has mixtures of several fluids, coloring optimization problems, and monolayers adsorbed on crystal surfaces. Herein, we will be interested in a particular case of the p-state planar Potts model (also known as clock model), which may be defined in terms of spin variables $\vec{S}_i$, characterized by two Cartesian components, $\vec{S}_i \equiv (S_{ix}, S_{iy})$. Let us introduce a quite general anisotropic Hamiltonian,

$$\begin{aligned}\mathcal{H}(\{h_{ix}, h_{iy}\}) = & - J_x \sum_{(ij)} S_{ix} S_{jx} - J_y \sum_{(ij)} S_{iy} S_{jy} - D_x \sum_{i=1}^{N} S_{ix}^2 - D_y \sum_{i=1}^{N} S_{iy}^2 \\ & - \sum_{i=1}^{N} h_{ix} S_{ix} - \sum_{i=1}^{N} h_{iy} S_{iy} \ , \end{aligned} \tag{1}$$

where $\sum_{(ij)}$ denote sums over all distinct pairs of spins ($i = 1, 2, \cdots N$), $J_x, J_y > 0$ are coupling constants, $D_x, D_y > 0$ represent anisotropy fields, whereas h_{ix} and h_{iy} are random magnetic fields acting, respectively, on each spin-variable Cartesian component. The p-state clock variables $\vec{S}_i$ are allowed to choose p directions in the xy plane, characterized by the components,

$$S_{ix} = \cos\theta_i \ ; \qquad S_{iy} = \sin\theta_i \ ; \qquad \theta_i = \frac{2\pi}{p}\, k_i \ ; \qquad (k_i = 0, 1, 2, \cdots, (p-1)) \ . \tag{2}$$

In the present work we will investigate the case $p = 4$ of the model above, for which the spin components in Eq. (2) may be expressed in terms of two Ising variables. In the next section we rewrite the Hamiltonian of Eq. (1) with these variables, discussing its properties both in the Cartesian and two-Ising representations; in this later case, we derive expressions for the free energy and order parameters. In Section III we analyze the phase diagrams of the model, by considering bimodal probability distributions for the random magnetic fields acting on the two sets of Ising variables; the physically distinct situations of fully correlated and uncorrelated fields in these sets of variables are investigated. It is shown that the second case, namely, independent probability distributions for each set of Ising variables, presents a rich variety of phase diagrams and may exhibit two distinct ferromagnetic phases, with curious phase boundaries, ordered critical points, tricritical,

and triple points. We also give heuristic domain-wall arguments for estimating the lower critical dimension, above which an ordered state should appear in the corresponding nearest-neighbor version of the model. Such a rich multicritical behavior is expected to be useful for describing magnetic systems, as well as other systems outside the area of magnetism, as occurs frequently in many other spin models. Finally, in Section IV we present our main conclusions.

II. THE TWO-ISING REPRESENTATION: FREE ENERGY AND EQUATIONS OF STATE

From now on we will be restricted to the case $p = 4$ of the model above; hence, the spin components in Eq. (2) may be expressed in terms of two Ising variables ($\tau_i = \pm 1$, and $\sigma_i = \pm 1$), through the relations

$$S_{ix} = \frac{1}{2}\left(\tau_i + \sigma_i\right); \qquad S_{iy} = \frac{1}{2}\left(\tau_i - \sigma_i\right) . \tag{3}$$

Considering isotropic coupling constants, i.e., $J_x = J_y$, the Hamiltonian of Eq. (1) can be rewritten as,

$$\mathcal{H}(\{h_i^\tau, h_i^\sigma\}) = -J\sum_{(ij)}\sigma_i\sigma_j - J\sum_{(ij)}\tau_i\tau_j - D\sum_{i=1}^{N}\tau_i\sigma_i - \sum_{i=1}^{N}h_i^\tau\tau_i - \sum_{i=1}^{N}h_i^\sigma\sigma_i \ , \tag{4}$$

where $J > 0$ ($J = J_x/2 = J_y/2$) favors ferromagnetic ordering in both Ising systems, and the random fields on each set of variables are related to those of Eq. (1) through $h_i^\tau = (h_{ix} + h_{iy})/2$ and $h_i^\sigma = (h_{ix} - h_{iy})/2$.

Comparing Eqs. (1) and (4) one sees that, through this change of variables, the anisotropy fields in the Cartesian-component representation result in $D = 2(D_x - D_y)$, leading to a coupling parameter between the two Ising systems. Hence, $D > 0$ favors a parallel alignment of the spins $\{\tau_i\}$ and $\{\sigma_i\}$, corresponding in Eq. (1) to a stronger anisotropy in the x-direction, whereas the antiparallel alignment of $\{\tau_i\}$ and $\{\sigma_i\}$ is preferred if $D < 0$, a consequence from a larger anisotropy field in the y-direction.

The analysis of Ref. [22] was inspired on a model for plastic crystals [15, 23–25], defined by means of two Ising variables, representing respectively, the translational and rotational degrees of freedom of a molecule. Certainly, these variables express very different characteristics of a molecule, and particularly, the rotational variables are expected to change more freely than the translational ones; for this reason, one introduces a random field acting only on the rotational degrees of freedom. In such a model, $h_i^\sigma = 0$ $(\forall i)$ was considered, which corresponds in the Hamiltonian of Eq. (1) to $h_{ix} = h_{iy}$ $(\forall i)$. In other systems, e.g., magnetic systems, random fields may result from a uniform external field applied in disordered magnetic media, as happens for diluted antiferromagnets [28–30]; in such cases one should have $h_{ix} \neq h_{iy}$ throughout the material, and one expects both random fields h_i^τ and h_i^σ to play an important role in the Hamiltonian of Eq. (4). This represents the situation to be considered in the present investigation.

Due to the infinite-range character of the interactions, one can write the Hamiltonian of Eq. (4) in the form

$$\mathcal{H}(\{h_i^\tau, h_i^\sigma\}) = -\frac{J}{2N}\left(\sum_{i=1}^{N}\sigma_i\right)^2 - \frac{J}{2N}\left(\sum_{i=1}^{N}\tau_i\right)^2 - D\sum_{i=1}^{N}\tau_i\sigma_i - \sum_{i=1}^{N}h_i^\tau\tau_i - \sum_{i=1}^{N}h_i^\sigma\sigma_i \ , \quad (5)$$

from which one may calculate the partition function associated with a particular realization of the fields $\{h_i^\tau, h_i^\sigma\}$,

$$Z(\{h_i^\tau, h_i^\sigma\}) = \mathrm{Tr}\exp\left[-\beta\mathcal{H}(\{h_i^\tau; h_i^\sigma\})\right] \ , \quad (6)$$

where $\beta = 1/(kT)$ and $\mathrm{Tr} \equiv \mathrm{Tr}_{\{\tau_i,\sigma_i=\pm1\}}$ indicates a sum over all spin configurations. One can now make use of the Hubbbard-Stratonovich transformation [5, 6] to linearize the quadratic terms, so that the dependence on the index i disappears,

$$Z(\{h^\tau, h^\sigma\}) = \frac{1}{\pi}\int_{-\infty}^{\infty} dx\, dy \exp(-x^2 - y^2)\{\mathrm{Tr}\exp[H(\tau, \sigma, h^\tau, h^\sigma)]\}^N \ , \quad (7)$$

where $H(\tau, \sigma, h^\tau, h^\sigma)$ is given by

$$H(\tau,\sigma,h^\tau,h^\sigma)=\sqrt{\frac{2\beta J}{N}}\;x\tau+\sqrt{\frac{2\beta J}{N}}\;y\sigma-\beta D\tau\sigma+\beta h^\tau\tau+\beta h^\sigma\sigma\;. \tag{8}$$

Performing the trace over the spins and defining new variables, related to the respective order parameters,

$$m_\tau=\sqrt{\frac{2kT}{JN}}\;x\;;\qquad m_\sigma=\sqrt{\frac{2kT}{JN}}\;y\;, \tag{9}$$

one obtains

$$Z(\{h^\tau,h^\sigma\})=\frac{\beta JN}{2\pi}\int_{-\infty}^{\infty}dm_\tau\,dm_\sigma\exp[N\mathcal{G}_{h^\tau,h^\sigma}(m_\tau,m_\sigma)]\;, \tag{10}$$

where

$$\begin{aligned}\mathcal{G}_{h^\tau,h^\sigma}(m_\tau,m_\sigma)\;=\;&-\frac{1}{2}\beta Jm_\tau^2-\frac{1}{2}\beta Jm_\sigma^2+\log\big\{2e^{\beta D}\cosh[\beta J(m_\tau+m_\sigma+h^\tau/J+h^\sigma/J)]\\&+\;2e^{-\beta D}\cosh[\beta J(m_\tau-m_\sigma+h^\tau/J-h^\sigma/J)]\big\}\;.\end{aligned} \tag{11}$$

As usual, one considers the thermodynamic limit ($N\to\infty$), and applies the saddle-point method to obtain $Z(\{h^\tau,h^\sigma\})$ [5, 6]. So, the free-energy density functional $f(m_\tau,m_\sigma)$ results from a quenched average of $-\mathcal{G}_{h^\tau,h^\sigma}(m_\tau,m_\sigma)$ in Eq. (11), over the joint probability distribution $P(h^\tau,h^\sigma)$,

$$f(m_\tau,m_\sigma)=\frac{1}{2}Jm_\tau^2+\frac{1}{2}Jm_\sigma^2-\frac{1}{\beta}\int_{-\infty}^{\infty}\int_{-\infty}^{\infty}dh^\tau dh^\sigma P(h^\tau,h^\sigma)\log Q(h^\tau,h^\sigma)\;, \tag{12}$$

with

$$\begin{aligned}Q(h^\tau,h^\sigma)\;=\;&2e^{\beta D}\cosh[\beta J(m_\tau+m_\sigma+h^\tau/J+h^\sigma/J)]\\&+\;2e^{-\beta D}\cosh[\beta J(m_\tau-m_\sigma+h^\tau/J-h^\sigma/J)]\;.\end{aligned} \tag{13}$$

If there is no correlation between the random fields $\{h_i^\tau\}$ and $\{h_i^\sigma\}$, the Hamiltonian in Eq. (4) presents a symmetry $D \to -D$, together with the inversion of one set of spin variables and its associated random field [e.g., $\sigma_i \to -\sigma_i$ and $h_i^\sigma \to -h_i^\sigma$ $(\forall i)$]. Since $D = 2(D_x - D_y)$ [from Eqs. (1) and (4)], this symmetry corresponds to two physically equivalent situations, namely, $D_x > D_y$ $(D > 0)$ and $D_x < D_y$ $(D < 0)$. The expression for the free energy above follows this symmetry [e.g., by considering $D \to -D$, $h^\sigma \to -h^\sigma$, and $m^\sigma \to -m^\sigma$ in Eq. (13)].

The extremization of the free-energy density above, with respect to the parameters m_τ and m_σ, yields the following equations of state,

$$m_\tau \;=\; \int_{-\infty}^{\infty}\int_{-\infty}^{\infty} dh^\tau dh^\sigma P(h^\tau,h^\sigma)\,\frac{R_+(h^\tau,h^\sigma)}{Q(h^\tau,h^\sigma)}\;, \tag{14}$$

$$m_\sigma \;=\; \int_{-\infty}^{\infty}\int_{-\infty}^{\infty} dh^\tau dh^\sigma P(h^\tau,h^\sigma)\,\frac{R_-(h^\tau,h^\sigma)}{Q(h^\tau,h^\sigma)}\;, \tag{15}$$

where

$$\begin{aligned} R_\pm(h^\tau,h^\sigma) \;&=\; e^{\beta D}\sinh[\beta J(m_\tau + m_\sigma + h^\tau/J + h^\sigma/J)] \\ &\pm\; e^{-\beta D}\sinh[\beta J(m_\tau - m_\sigma + h^\tau/J - h^\sigma/J)]\;. \end{aligned} \tag{16}$$

Now, in order to proceed with the calculations, one has to define the joint probability distribution $P(h^\tau,h^\sigma)$, which appears in Eqs. (12), (14), and (15). Herein, we will consider the quite interesting (characterized by a rich critical behavior) case of bimodal probability distributions [8] in two extreme situations, namely, fully correlated, and totally uncorrelated fields h^τ and h^σ.

In the first case we will consider $h^\tau = h^\sigma = h$, with h following

$$P(h) = \frac{1}{2}\,\delta(h - h_0) + \frac{1}{2}\,\delta(h + h_0)\;. \tag{17}$$

This represents a situation where in each position i the fields $\{h_i^\tau\}$ and $\{h_i^\sigma\}$ are the same, and may be associated to effects due to the randomnesses and anisotropies of the

medium only. In the Cartesian-component representation it corresponds to $h_{iy} = 0$, so that $h_i^\tau = h_i^\sigma = h_{ix}/2$ $(\forall i)$. Due to this correlation in the random fields, the symmetry of the Hamiltonian in Eq. (4), $D \to -D$, together with the inversion of one set of spin variables and its associated random field, is broken. Moreover, since $h_{iy} = 0$, this case yields two physically distinct situations, namely, $D > 0$ $(D_x > D_y)$ and $D < 0$ $(D_x < D_y)$.

For $D > 0$ the system may be described by a single order parameter m, such that $m = m_\tau = m_\sigma$, leading to the following free energy,

$$\begin{aligned} f &= Jm^2 - \frac{1}{2\beta}\log[2\exp(\beta D)\cosh[2\beta J(m + h_0/J)] + 2\exp(-\beta D)\cosh[2\beta J(m + h_0/J)]] \\ &- \frac{1}{2\beta}\log[2\exp(\beta D)\cosh[2\beta J(m - h_0/J)] + 2\exp(-\beta D)\cosh[2\beta J(m - h_0/J)]] \ , \end{aligned} \tag{18}$$

and equation of state,

$$\begin{aligned} m &= \frac{1}{2}\left[\frac{\sinh[2\beta J(m + h_0/J)]}{\cosh[2\beta J(m + h_0/J)] + \exp(-2\beta D)}\right] \\ &+ \frac{1}{2}\left[\frac{\sinh[2\beta J(m - h_0/J)]}{\cosh[2\beta J(m - h_0/J)] + \exp(-2\beta D)}\right] \ . \end{aligned} \tag{19}$$

On the other hand, for $D < 0$ one considers $m = m_\tau = -m_\sigma$, which yields

$$f = Jm^2 - \frac{1}{\beta}\log[2\exp(\beta D)\cosh(2\beta h_0) + 2\exp(-\beta D)\cosh(2\beta Jm)] \ , \tag{20}$$

and

$$m = \frac{\sinh(2\beta Jm)}{\exp(2\beta D)\cosh(2\beta h_0) + \cosh(2\beta Jm)} \ . \tag{21}$$

As a second possibility for the random fields, we take h^τ and h^σ uncorrelated, so the joint probability distribution is given by

$$P(h^\tau, h^\sigma) = P(h^\tau)P(h^\sigma) \ , \tag{22}$$

and we consider

$$P(h^{\sigma}) = \frac{1}{2}\,\delta(h^{\sigma} - h_0) + \frac{1}{2}\,\delta(h^{\sigma} + h_0)\ , \tag{23}$$

$$P(h^{\tau}) = \frac{1}{2}\,\delta(h^{\tau} - h_0) + \frac{1}{2}\,\delta(h^{\tau} + h_0)\ , \tag{24}$$

as the probability distribution functions for the random fields acting on each Ising system.

In the Cartesian-component representation this typifies a situation characterized by local anisotropies, leading to $h_{ix} \neq h_{iy}$, so that both random fields, $h_i^{\tau} = (h_{ix} + h_{iy})/2$ and $h_i^{\sigma} = (h_{ix} - h_{iy})/2$, play important roles separately. These realizations, where in each position i one has independent fields, $\{h_i^{\tau}\}$ and $\{h_i^{\sigma}\}$, may result from randomnesses of the medium, as well as from other possible effects (e.g., from the remaining spin variables), such as to act distinctly on the systems $\{\tau_i\}$ and $\{\sigma_i\}$. As mentioned before, this case follows the symmetry $D \to -D$ in Eq. (4), and so an investigation of $D \geq 0$ becomes sufficient.

After perfoming the integrals in Eqs. (12), (14), and (15), one can show that $m_{\tau} = m_{\sigma}$ appears as a solution (due the symmetry of the Hamiltonian in Eq. (4), the equivalent solution $m_{\tau} = -m_{\sigma}$ appears in the case $D < 0$). It should be mentioned that, in our numerical analysis, we did not find any physically distinct solution from this one for finite temperatures; however, as will be shown below, solutions characterized by $m_{\tau} \neq m_{\sigma}$ appear at $T = 0$. Hence, for $T > 0$, similarly to the previous case (fully correlated random fields), the system will be described by a single order parameter m, with $m = m_{\tau} = m_{\sigma}$. The resulting expressions for the free energy and order parameter are

$$\begin{aligned} f = Jm^2 \ &- \ \frac{1}{4\beta}\log[2\exp(\beta D)\cosh[2\beta J(m + h_0/J)] + 2\exp(-\beta D)] \\ &- \ \frac{1}{4\beta}\log[2\exp(\beta D)\cosh[2\beta J(m - h_0/J)] + 2\exp(-\beta D)] \\ &- \ \frac{1}{2\beta}\log[2\exp(\beta D)\cosh(2\beta Jm) + 2\exp(-\beta D)\cosh(2\beta h_0)]\ , \end{aligned} \tag{25}$$

$$
\begin{aligned}
m \;=\; & \frac{1}{4}\left[\frac{\sinh[2\beta J(m+h_0/J)]}{\cosh[2\beta J(m+h_0/J)]+\exp(-2\beta D)}\right] \\
+\; & \frac{1}{4}\left[\frac{\sinh[2\beta J(m-h_0/J)]}{\cosh[2\beta J(m-h_0/J)]+\exp(-2\beta D)}\right] \\
+\; & \frac{1}{2}\left[\frac{\sinh(2\beta Jm)}{\cosh(2\beta Jm)+\exp(-2\beta D)\cosh(2\beta h_0)}\right] \;. \qquad (26)
\end{aligned}
$$

In the next section we present and discuss the phase diagrams of the model, considering these two choices for the the joint probability distribution $P(h^\tau, h^\sigma)$. In both cases, the equation of state for the single order parameter may be expanded as a power series in m, in the neighborhood of a continuous (second-order) phase transition,

$$
m = A_1(\beta, D, h_0)m + A_3(\beta, D, h_0)m^3 + A_5(\beta, D, h_0)m^5 + A_7(\beta, D, h_0)m^7 + \cdots \;. \qquad (27)
$$

As usual, the continuous frontiers can be obtained by solving numerically the equation $A_1 = 1$, provided that $A_3 < 0$. In cases where these frontiers end at a tricritical point, such a point is obtained by setting $A_1 = 1$ and $A_3 = 0$, conditioned to $A_5 < 0$. Furthermore, the so-called fourth-order critical point, after which tricritical points do not occur (as a single critical point), is located by $A_1 = 1$, $A_3 = 0$, and $A_5 = 0$, provided that $A_7 < 0$. The first-order critical frontiers are obtained by standard Maxwell constructions; nevertheless, numerical analysis can produce spurious solutions, so one must always check if the free energy is minimized.

All phase diagrams will be represented in terms of dimensionless variables, by rescaling conveniently the energy parameters of the system, namely, kT/J, h_0/J, and D/J. Both ordered ($m \neq 0$) and disordered ($m = 0$) phases have appeared in our analysis, and as usual, they will be labelled by **F** (ferromagnetic) and **P** (paramagnetic) phases, respectively. In some of our phase diagrams we find two distinct ferromagnetic phases (to be labelled by $\mathbf{F_1}$ and $\mathbf{F_2}$), separated by a first-order phase transition, characterized by a jump in their respective magnetizations, $m_1 \neq m_2$. It should be emphasized that the solution $m_\tau = m_\sigma$ still holds throughout both phases $\mathbf{F_1}$ and $\mathbf{F_2}$.

A wide variety of critical points appeared in our analysis, and herein we follow the classification due to Griffiths [31]: (i) a tricritical point signals the encounter of a continuous frontier with a first-order line with no change of slope; (ii) an ordered critical point corresponds to an isolated critical point inside the ordered region, terminating a first-order line that separates two distinct ordered phases; (iii) a triple point, where three distinct phases coexist, signals the encounter of three first-order critical frontiers; (iv) a critical end point, where three phases coexist, corresponding to the intersection of a continuous line that separates the paramagnetic from one of the ferromagnetic phases, a first-order line separating the paramagnetic and the other ferromagnetic phase, and a first-order line separating the two ferromagnetic phases; (v) a multicritical point, where several phases coexist. The location of the critical points defined in (ii)–(v), as well as of the first-order critical frontiers, were determined by a numerical analysis of the free-energy minima. In the phase diagrams we shall use distinct symbols and representations for the critical points and frontiers, as described below.

- Continuous (second-order) critical frontier: continuous line.
- First-order critical frontier: dotted line.
- Tricritical point: located by a black circle.
- Fourth-order critical point: located by an empty square.
- Ordered critical point: located by a black asterisk.
- Triple point: located by an empty triangle.
- Critical end point: located by a black triangle.
- Multicritical point: located by an empty diamond.

These types of behavior appear frequently in many real systems, e.g., magnetic compounds and fluid mixtures [1, 32–34]; next, we describe some concrete examples. (i) Multicritical phenomena occur along the surface of magnetic systems, if the atomic interactions of the surface layer differ significantly from those of the bulk [32]. In these systems the corresponding phase diagrams may present distinct ordered phases, as well

as regions of coexisting ordered-ordered and ordered-disordered states. Along these coexistence regions, evidence of bicritical, tricritical, and triple points, have been found. (ii) A first-order critical line in the plane magnetic field versus temperature, terminating at a critical-end point, has been detected in the magnetic compound $MnFeAs_yP_{1-y}$, for $y = 0.26$ [35]. (iii) Some binary compounds, like $PrGe_{1.6}$ and $CeGe_{1.6}$ (rare-earth germanides), have shown evidence of a coexistence of two distinct ferromagnetic phases [36]; in particular, the former compound has shown Pr atoms at given sites with a substantially larger magnetic moment than those of Pr atoms at other sites [37]. The coexisitence of two ferromagnetic phases represents one of the main results of the present work. (iv) Diluted antiferromagnets in the presence of a uniform field are considered as physical representations of a ferromagnet under random fields [28–30]; as a well-known example one could mention the compound $Fe_xMg_{1-x}Cl_2$. A curious crossover from a first-order to a second-order phase transition has been observed by decreasing x (this crossover is estimated to happen for $x \approx 0.6$) [38, 39]. One expects such an effect to occur, not as an abrupt change, but rather through the appearance of some type of multicritical behavior; hence, a fine tunning of the parameter x in the range $0.6 \leq x \leq 1.0$ is highly desirable, and should indicate interesting aspects. (v) Fluid mixtures may be, in many cases, mapped into magnetic models, in such a way that discrete variables characterized by more than two states, like those of the present investigation, are necessary for an appropriate description of some ternary and quaternary fluid mixtures. These mixtures are good candidates for exhibiting multicritical phenomena [1, 33, 34]; it should be mentioned that tricritical points have been observed in several multicomponent-fluid mixtures (a vast list of them may be found in Ref. [40]).

Before starting a detailed quantitative investigation of the phase diagrams and critical points of the model, we first carry out a ground-state analysis, based on the Hamiltonian of Eq. (4) [or equivalently, in Eq. (5)]. One notices important competing contributions in the Hamiltonian of Eq. (5), namely, the two quadratic ones, associated with ferromagnetic orderings of each system, characterized by a coupling J, random fields acting on each Ising system with an intensity h_0, and the coupling between the two systems, given by an intensity $|D|$. In the limit where the random field dominates ($h_0 \gg J$), one expects a disordered state (**P** phase), where the quadratic terms yield zero to the total

internal energy U. However, the resulting energy depends strongly on the coupling D, and particularly in the case of fully correlated random fields, on the sign of D, i.e., through a tendency for aligning the two systems parallel to each other if $D > 0$, or anti-parallel if $D < 0$. Hence, for the **P** phase one has several possible situations, as described next. (a) For uncorrelated random fields, the two systems become disordered independently, so that $(u/J) = -(2h_0/J)$, for both signs of D. (b) For fully correlated fields and $D > 0$, each system becomes disordered, but aligned with respect to each other, leading to $(u/J) = -(2h_0/J) - (D/J)$; however, for $D < 0$ each system becomes disordered and anti-parallel to each other, so that the random-field contribution cancels out, leading to $(u/J) = (D/J)$. Another important regime concerns the one where the ferromagnetic ordering becomes relevant, prevailing over the random-field contributions ($h_0 \ll J$). Considering in the present analysis only the zero-temperature ferromagnetic ordering with maximum magnetization, each quadratic term in the Hamiltonian of Eq. (5) contributes with $-JN/2$ to the total internal energy. Therefore, one obtains the internal energy per particle $(u/J) = -1 - (D/J)$, for uncorrelated fields (any D), as well for fully correlated fields and $D > 0$. However, the case of fully correlated fields and $D < 0$ has shown to be more subtle, deserving a careful quantitive study, as will be discussed in the next section. On the basis of this analysis, one may equate the corresponding internal energies to obtain the zero-temperature first-order critical frontiers separating the paramagnetic and ferromagnetic phases, for fully correlated random fields ($D > 0$), as well as for uncorrelated fields (any D). As will be seen in the next section, in the first case one gets the zero-temperature critical field $(h_{0c}/J) = 1/2$ (any $D > 0$), whereas in the latter, the critical frontier $(D/J) = (2h_0/J) - 1$ separates the phases **P** and $\mathbf{F_1}$. However, the most interesting and rich critical behavior will appear in the case of uncorrelated fields, when the parameters J, D, and h_0, in the Hamiltonian of Eq. (5), become of the same order of magnitude, i.e., $(D/J) \approx (h_0/J)$, where a multicritical point emerges; such a zero-temperature point will have an important influence on the finite-temperature phase diagrams.

III. RESULTS AND DISCUSSIONS

A. Correlated Fields

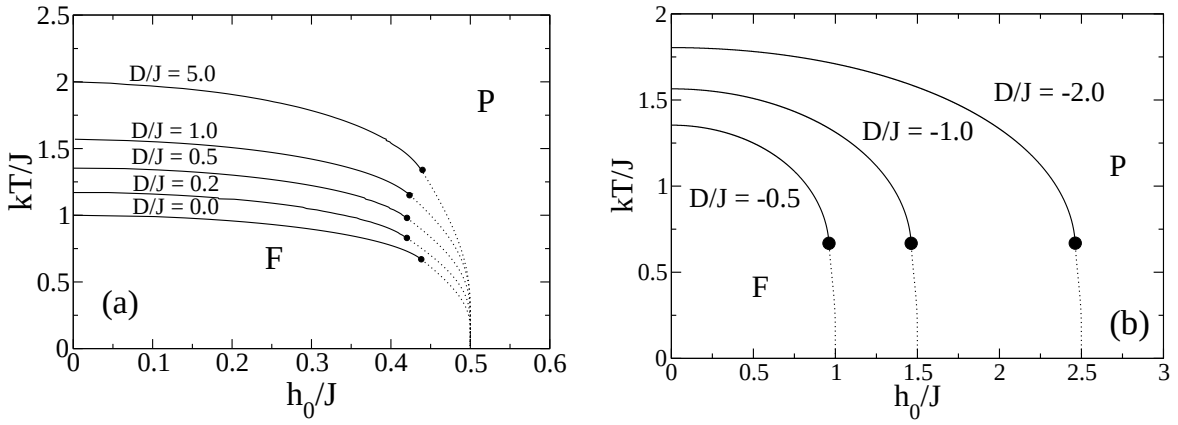

FIG. 1: Phase diagram in the plane of conveniently rescaled variables, kT/J (dimensionless temperature) versus h_0/J (dimensionless field strength), in the case of fully correlated fields h^τ and h^σ. (a) Typical values of the dimensionless coupling $(D/J) \geq 0$; (b) Typical negative values of the dimensionless coupling D/J.

As discussed above, for fully correlated fields ($h^\tau = h^\sigma = \pm h_0$) one needs to analyze separately the different signs of the coupling parameter D; the free energy and order parameter are given, respectively, by Eqs. (18) and (19) in the case $D > 0$, whereas for $D < 0$ one should use Eqs. (20) and (21). The associated phase diagrams are shown in Fig. 1 in the plane of dimensionless variables kT/J versus h_0/J. From the qualitative point of view, all phase diagrams are similar to the one of an Ising ferromagnet in the presence of a bimodal random field [8] (which corresponds to the case $D = 0$ in Fig. 1(a), i.e., two independent Ising models). In analogy to Ref. [8], the two phases **P** and **F** are separated by a continuous frontier at high temperatures, followed by a first-order one for lower temperatures; these two critical lines meet with no change of slope at a tricritical point (black circle).

The quantitative differences of the phase diagrams presented in Figs. 1(a) and 1(b) correspond to the enlargement of phase **F** as $|D|$ increases, characterized by solutions $m > 0$, where $m = m_\tau = m_\sigma$ $(D > 0)$, or $m = m_\tau = -m_\sigma$ $(D < 0)$. Indeed, for

$(h_0/J) = 0$, the critical temperature is determined in both cases by solving the equation

$$\frac{kT_c}{J} = \frac{2}{1+\exp(-2|D|/kT_c)} \ , \tag{28}$$

which comes from setting the coefficient $A_1(\beta, D, 0) = 1$ in the Landau expansion [cf. Eq. (27)] for the order parameter given in Eq. (19) ($D > 0$), or in Eq. (21) ($D < 0$). In both cases one sees that $(kT_c/J) \to 2$, for sufficiently large values of $|D|$, as shown in Fig. 1. From Eq. (28) one notices that the symmetry $D \to -D$ is recovered in this particular limit, as expected from the Hamiltonian in Eq. (4) in the absence of random fields.

However, at zero temperature the system is sensitive to the sign of D, and the first-order phase transitions are obtained by equating the free energies (i.e., internal energies per particle, u) of the phases **P** and **F**. The corresponding critical points h_{0c}/J may be calculated analytically either from Eq. (18),

$$u_{\mathbf{F}} = -(J+D); \quad u_{\mathbf{P}} = -(2h_0 + D); \quad \Rightarrow \quad \frac{h_{0c}}{J} = \frac{1}{2}; \quad (D > 0), \tag{29}$$

or from Eq. (20),

$$u_{\mathbf{F}} = J - (D + 2h_0); \quad u_{\mathbf{P}} = D; \quad \Rightarrow \quad \frac{h_{0c}}{J} = \frac{1}{2} - \frac{D}{J} \quad (D < 0). \tag{30}$$

The zero-temperature critical points of Eqs. (29) and (30) show a significant difference as one changes the sign of the coupling parameter D. From Eq. (4) one sees that for $D = 0$ one has two independent Ising models, and each of them presents a zero-temperature phase transition at $(h_{0c}/J) = 1/2$, following the Ising ferromagnet in the presence of a bimodal random field [8]. In Fig. 1(a) this critical point remains unchanged by introducing a positive coupling between the two Ising systems. In the Cartesian-component representation, one should remind that the present situation, $h_i^\sigma = h_i^\tau$, yields $h_{iy} = 0$, whereas $D = 2(D_x - D_y)$, so that $D > 0$ ($D < 0$) corresponds to $D_x > D_y$ ($D_x < D_y$). Hence, the critical points for $D > 0$ are associated typically with a random-field phase transition in x-direction only, and increasing the anisotropy in this direction does not

change the zero-temperature critical point. However, a negative D leads to a stronger anisotropy in the y-direction, along which there is no random field. Since the effect of a random field consists in decreasing the critical temperature with respect to the one for $h_0 = 0$, the preference for the y-direction yields a persistence of the **F** phase for larger values of h_0, leading to a shift of the zero-temperature critical point in Fig. 1(b) according to $(h_{0c}/J) = 1/2 - (D/J)$.

B. Uncorrelated Fields

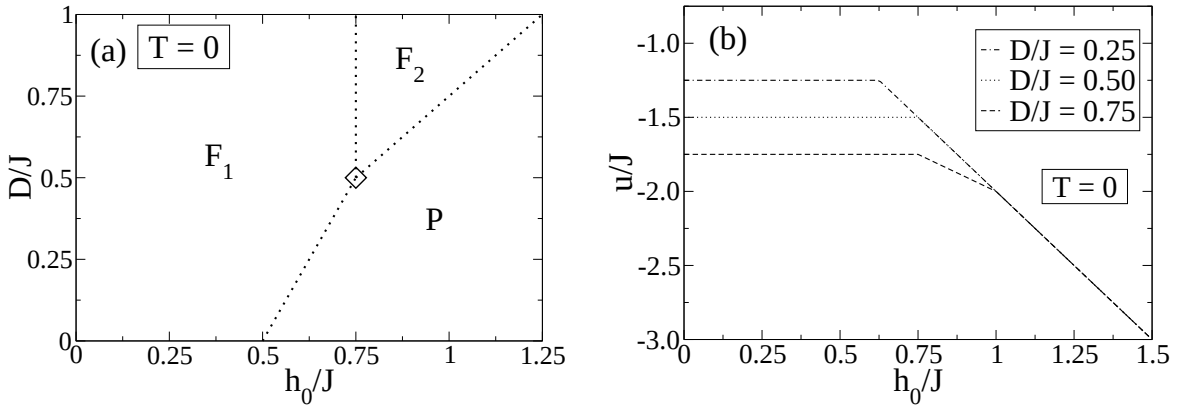

FIG. 2: Zero-temperature analysis of the model defined in Eq. (4), in the case of uncorrelated fields h_i^τ and h_i^σ. (a) Phase diagram in the plane of dimensionless variables D/J versus h_0/J; all critical frontiers are first order, whereas at the multicritical point (represented by an empty diamond) one has a coexistence of several solutions, as described in the text. (b) The dimensionless internal energy per particle u/J is shown versus h_0/J for typical values of D/J; the two limiting values, i.e., $(u/J) = -1 - (D/J)$ (for $h_0 \ll J$) and $(u/J) = -(2h_0/J)$ (for $h_0 \gg J$), predicted in the ground-state analysis at the end of the previous section, are verified.

According to the discussion of the previous section, this case presents the symmetry $D \to -D$ in Eq. (4), so that from now on we restrict ourselves to $D \geq 0$. As it will be seen throughout this section, the condition of uncorrelated fields leads to a rich criticality, and due to this, we first carry out an analysis at zero temperature. In Fig. 2(a) we exhibit the phase diagram at zero temperature in the plane of dimensionless variables D/J versus h_0/J, where three first-order critical frontiers delimit the phases **P**, $\mathbf{F_1}$, and $\mathbf{F_2}$.

These phases correspond to three different values of the order parameter $m = m_\tau = m_\sigma$ that appear as solutions of Eq. (26), minimizing the Hamiltonian given in Eq. (4): $m = 0$ (phase $\mathbf{P}$), $m = 1$ (phase $\mathbf{F_1}$), and $m = 1/2$ (phase $\mathbf{F_2}$). For $0 \leq (D/J) < 1/2$ one has the first two phases only, whereas for $(D/J) \geq 1/2$ all three phases become possible. In the former case, the phases $\mathbf{P}$ and $\mathbf{F_1}$ are separated by a critical frontier given by $(D/J) = (2h_0/J) - 1$. In the later $[(D/J) \geq 1/2]$, one has two first-order frontiers, represented by the vertical line $(h_0/J) = 3/4$ that separates the ordered phases $\mathbf{F_1}$ and $\mathbf{F_2}$, and the line $(D/J) = (h_0/J) - 1/4$ that divides the ordered phase $\mathbf{F_2}$ from the paramagnetic one. However, the most interesting aspect of the phase diagram of Fig. 2 corresponds to the multicritical point, where these three lines meet at $[(h_0/J) = 0.75, (D/J) = 0.5]$ (represented by an empty diamond). Curiously, the order parameters m_τ and m_σ yield a coexistence of several solutions at this point (some of them breaking the equality of these order parameters): $(m_\tau, m_\sigma) = \{(-1,-1); (-1/2,-1/2); (0,0); (0,1/2); (0,-1/2); (-1/2,0); (1/2,0); (1/2,1/2); (1,1)\}$). In Fig. 2(b) we represent the dimensionless internal energy per particle u/J versus h_0/J, for typical values of D/J (increasing values of D/J, from top to bottom). One notices that u/J takes a constant value for sufficiently small values of h_0/J (throughout phase $\mathbf{F_1}$), or decreases linearly with h_0/J (throughout phases $\mathbf{F_2}$ and $\mathbf{P}$), changing its slope at each critical frontier. According to the ground-state analysis at the end of the previous section, one has two limiting values for the internal energy, namely, $(u/J) = -1 - (D/J)$ (for $h_0 \ll J$) and $(u/J) = -(2h_0/J)$ (for $h_0 \gg J$), which are precisely those represented in Fig. 2(b), associated respectively, with phases $\mathbf{F_1}$ and $\mathbf{P}$. Indeed, by equating these two energies, one obtains the critical frontier separating such phases, i.e., $(D/J) = (2h_0/J) - 1$.

In Fig. 3 we present phase diagrams for two typical values of the dimensionless coupling between the two sets of Ising variables, namely, $(D/J) = 0.25$ and $(D/J) = 0.3535$, with critical frontiers separating the ferromagnetic phase $\mathbf{F_1}$ (sufficiently small values of kT/J and h_0/J) from the paramagnetic phase $\mathbf{P}$. In Fig. 3(a) one notices that the value of the coupling D/J is not sufficiently strong to change qualitatively the phase diagram of an Ising ferromagnet in the presence of a bimodal random field [8], where one finds a tricritical point signalling the encounter of the continuous frontier (high temperatures)

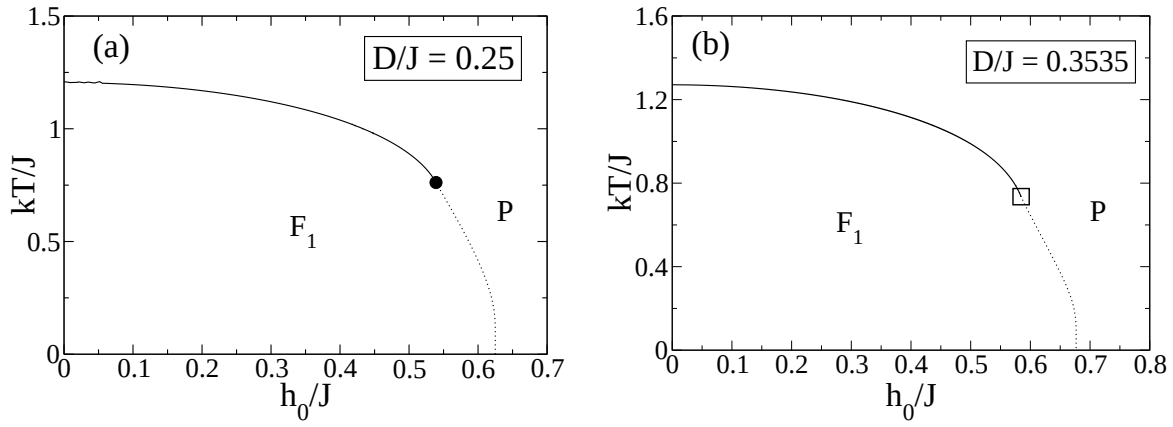

FIG. 3: Phase diagrams are exhibited for two typical values of the dimensionless coupling between the two Ising variables D/J, in the plane of conveniently rescaled variables, kT/J (dimensionless temperature) versus h_0/J (dimensionless field strength). (a) Case $(D/J) = 0.25$, showing a tricritical point (black circle), where a continuous frontier (high temperatures) meets a first-order critical frontier (low temperatures); we shall refer to this type of phase diagram as topology I. (b) Case $(D/J) = 0.3535$, where the empty square denotes a fourth-order critical point, which represents the limit for the appearance of the single tricritical point shown in (a) (see text).

with a first-order critical frontier (low temperatures). In this case, the only quantitative effect concerns an enlargement of phase $\mathbf{F_1}$ by increasing D/J; such a phase diagram will be referred from now on as topology I, and it appears for $0 < (D/J) < 0.3535$. Such a topology ends up at $(D/J) = 0.3535$, where the tricritical point turns into a fourth-order critical point [located at $(h_0/J) = 0.585; (kT/J) = 0.735$ and represented by the empty square in Fig. 3(b)]. Fourth-order critical points were found in other disordered spin models, like those treated in references [11, 12, 20, 21]; they are sometimes entitled in the literature as "vestigial" tricritical points, because they delimit the existence of those critical points [12].

For $(D/J) > 0.3535$ the additional ordered phase $\mathbf{F_2}$ arises, although for a certain range of values of D/J it may occupy a small part of the phase diagram, as shown in Fig. 4(a) for the case $(D/J) = 0.45$. In the inset of Fig. 4(a) one sees the piece of the first-order critical frontier that separates the phases $\mathbf{F_1}$ and $\mathbf{F_2}$, delimiting phase $\mathbf{F_2}$, from the critical end

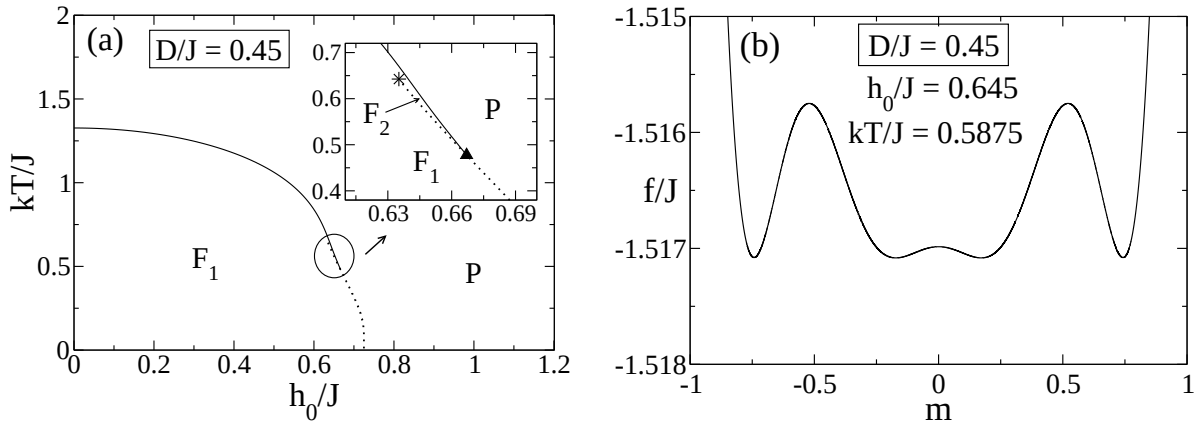

FIG. 4: (a) Phase diagram for a typical value of the dimensionless coupling between the two Ising variables, $(D/J) = 0.45$, in the plane of conveniently rescaled variables, kT/J (dimensionless temperature) versus h_0/J (dimensionless field strength). The ordered phase $\mathbf{F_2}$ appears in a small part of the phase diagram, as shown in the enlargement of the inset; the black triangle and the asterisk represent a critical end point and an ordered critical point, respectively; we shall refer to this type of phase diagram as topology II. (b) The dimensionless free energy is plotted versus the dimensionless order parameter, for a point of the phase diagram located at $[(h_0/J) = 0.6450; (kT/J) = 0.5875]$, belonging to the first-order frontier shown in the inset of (a), which divides the phases $\mathbf{F_1}$ and $\mathbf{F_2}$.

point (represented by a black triangle) to the ordered critical point (represented by an asterisk). From now on, we shall refer to this type of phase diagram as topology II, and as it will be discussed next, this topology applies for $0.3535 < (D/J) < 0.470$. In this case, the border of the $\mathbf{P}$ phase is given by a continuous part (high temperatures) that ends up at a critical end point, being followed by a first-order critical frontier (low temperatures). For temperatures right above the critical end point, one can go continuously from the $\mathbf{P}$ phase to $\mathbf{F_2}$; however, most of the $\mathbf{P}$ border is shared with the $\mathbf{F_1}$ phase, as shown in Fig. 4(a). In Fig. 4(b) we plot the dimensionless free energy versus the dimensionless order parameter, for a point of the phase diagram belonging to the first-order frontier shown in the inset of (a), dividing phases $\mathbf{F_1}$ and $\mathbf{F_2}$; one sees clearly the coexistence of two different values of $|m|$, typical of a first-order criticality.

By increasing gradually D/J we have verified that the critical end point of Fig. 4(a)

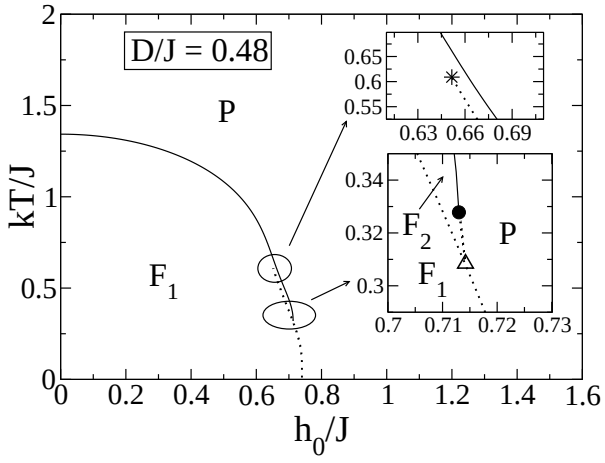

FIG. 5: Phase diagram for a typical value of the dimensionless coupling between the two Ising variables, $(D/J) = 0.48$, in the plane of conveniently rescaled variables, kT/J (dimensionless temperature) versus h_0/J (dimensionless field strength). The ordered phase $\mathbf{F_2}$ and critical points are shown in the insets, where we have enlarged two important regions of the phase diagram, represented by ellipses. In the lower inset one sees a triple point (empty triangle) and a tricritical point (black circle), which emerged from the critical end point of Fig. 4(a). In the upper inset we show the ordered critical point signalling the end of phase $\mathbf{F_2}$. We shall refer to this type of phase diagram as topology III.

disappears, giving rise to two other critical points, namely, a triple and a tricritical one. This is shown in Fig. 5 where we present the phase diagram for $(D/J) = 0.48$; the ordered phase $\mathbf{F_2}$, as well as the critical points are shown in the insets, through enlargements of two relevant parts of the critical region. In order to determine the upper limit associated with topology II, we had to estimate numerically the value of D/J for which the tricritical point emerges, leading to topology III. We have found that this occurs for $(D/J) = 0.471 \pm 0.001$, in the sense that topology II holds clearly for $(D/J) = 0.470$, whereas topology III applies for $(D/J) = 0.472$. In this later topology, the border of the $\mathbf{P}$ phase presents a rather rich critical behavior, whereas the critical frontier between the two ordered phases ($\mathbf{F_1}$ and $\mathbf{F_2}$) is first-order, terminating in an ordered critical point, similarly to the one shown in Fig. 4(a). The border of the $\mathbf{P}$ phase is composed by a continuous part (high temperatures) that ends up at a tricritical point, being followed by a small first-order critical frontier down to the triple point, below which a first-order phase transition separates phases $\mathbf{P}$

and $\mathbf{F_1}$. The frontier between phases $\mathbf{P}$ and $\mathbf{F_2}$ is either continuous (above the tricritical point), or first-order (between the tricritical and triple points). The region of the two insets of Fig. 5 suggests that such a rich critical behavior should be influenced by the zero-temperature multicritical point (located at $[(h_0/J) = 0.75, (D/J) = 0.5]$ in Fig. 2), where one has a coexistence of nine different solutions for the order parameters.

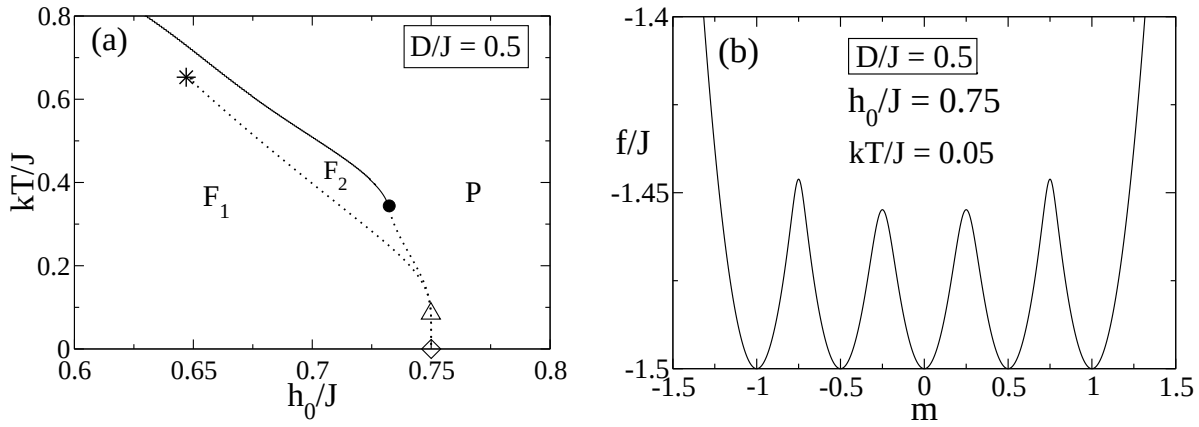

FIG. 6: (a) Phase diagram for the dimensionless coupling $(D/J) = 0.5$, in the plane of conveniently rescaled variables, kT/J (dimensionless temperature) versus h_0/J (dimensionless field strength). The two ordered phases ($\mathbf{F_1}$ and $\mathbf{F_2}$) are separated by a first-order critical frontier that terminates at an ordered critical point (represented by an asterisk). The border of the $\mathbf{P}$ phase presents a tricritical (black circle) and a triple point (empty triangle) at finite temperatures, whereas at zero temperature one finds the multicritical point of Fig. 2 (represented by an empty diamond). We shall refer to this type of phase diagram as topology IV. (b) The dimensionless free energy is plotted versus the dimensionless order parameter, for a point of the phase diagram located at $[(h_0/J) = 0.75; (kT/J) = 0.05]$, belonging to the low-temperature first-order frontier delimited by the triple and multicritical points.

For $(D/J) = 0.5$, topology III ends up through the appearance of the multicritical point at zero temperature, as shown in Fig. 6(a) (to be referred hereafter as topology IV). This point (represented by the empty diamond) corresponds to the multicritical point already exhibited in Fig. 2, and, as expected, it occurs only for $(D/J) = 0.5$. In this sense, topology III applies for $0.472 \leq (D/J) < 0.5$, whereas topology IV holds only for $(D/J) = 0.5$. Comparing Figs. 5 and 6(a) one notices, besides the zero-temperature

multicritical point, an enlargement of phase $\mathbf{F_2}$, essentially due to fact that the triple point is now located at a much lower temperature, maintaining the topological structure shown in the insets of Fig. 5. To illustrate the low-temperature critical behavior, in Fig. 6(b) we plot the dimensionless free energy versus the dimensionless order parameter, for a point of the phase diagram belonging to the first-order frontier delimited by the triple and the multicritical points. There, the free energy exhibits solutions corresponding to the two ordered phases ($\mathbf{F_1}$ and $\mathbf{F_2}$) coexisting with the disordered phase one ($m = 0$). We verified that when this first-order frontier approaches zero temperature (close to the multicritical point), four local minima, characterized by higher values of f/J, corresponding to $(m_\tau, m_\sigma) = \{(0, 1/2); (0, -1/2); (-1/2, 0); (1/2, 0)\}$, approach the five coexisting global minima shown in Fig. 6(b), corresponding to $(m_\tau = m, m_\sigma = m) = \{(-1, -1); (-1/2, -1/2); (0, 0); (1/2, 1/2); (1, 1)\}$. Accordingly, nine phases will coexist when the lower first-order curve touches the multicritical point at zero temperature. Therefore, this corresponds to the only point at which one finds solutions with $m_\tau \neq m_\sigma$, as discussed in the zero-temperature phase diagram of Fig. 2.

In Fig. 7 we exhibit phase diagrams for two typical values of the dimensionless coupling D/J [with $(D/J) > 0.5$], corresponding to topology V. In contrast to topologies II–IV, one sees clearly that the first-order frontier dividing phases $\mathbf{F_1}$ and $\mathbf{F_2}$ appears now shifted from the one that divides $\mathbf{F_2}$ and $\mathbf{P}$. This aspect has to do with the zero-temperature phase diagram presented in Fig. 2, where these two frontiers for $T = 0$ start, respectively, at $(h_0/J) = 0.75$ and $(h_0/J) = (D/J) + 1/4$, for $(D/J) > 0.5$. The border of the $\mathbf{P}$ phase is now characterized by a change of concavity, as well as by a single tricritical point, signalling the encounter of the continuous part of the frontier with the first-order one; this later aspect reminds topology I [cf. Fig. 3(a)]. However, as already mentioned, the tricritical point does not appear as the sole critical point of the phase diagram, an effect that occurs only up to $(D/J) = 0.3535$, where the fourth-order critical point emerges, as shown in Fig. 3(b). We have not found any qualitative change in the phase diagram of topology V by increasing further D/J; in fact, comparing Figs. 7(a) and (b), one notices that the effect of increasing D/J corresponds to an enlargement of phase $\mathbf{F_2}$, associated with a shift of the low-temperature first-order critical frontier starting at $(h_{0c}/J) = (D/J) + 1/4$, for zero temperature. A similar effect was verified in the case $D < 0$ of fully correlated fields

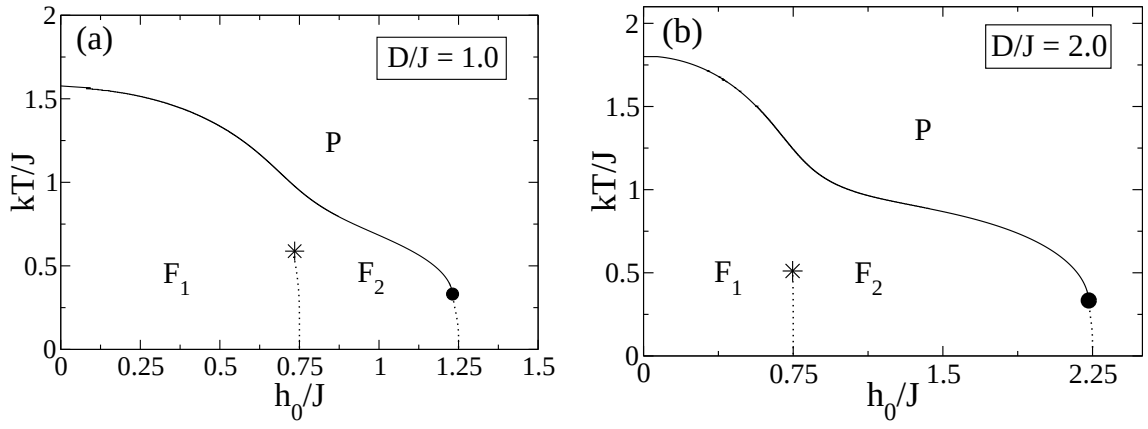

FIG. 7: Phase diagrams for two typical values of the dimensionless coupling D/J [with $(D/J) > 0.5$], in the plane of conveniently rescaled variables, kT/J (dimensionless temperature) versus h_0/J (dimensionless field strength). The two ordered phases ($\mathbf{F_1}$ and $\mathbf{F_2}$) are separated by a first-order critical frontier that terminates at an ordered critical point (represented by an asterisk). The border of the $\mathbf{P}$ phase presents a tricritical point only (black circle). (a) Case $(D/J) = 1.0$; (b) Case $(D/J) = 2.0$; we shall refer to this type of phase diagram as topology V. In these cases, according to the phase diagram at zero-temperature (cf. Fig. 2), the first-order frontier separating phases $\mathbf{F_1}$ and $\mathbf{F_2}$ starts at $(h_0/J) = 0.75$, whereas the one dividing phases $\mathbf{F_2}$ and $\mathbf{P}$ starts at $(h_0/J) = (D/J) + 1/4$.

[cf. Fig. 1(b)], where the zero-temperature critical point was shown to move according to $(h_{0c}/J) = |D/J| + 1/2$.

C. Domain-Wall Analysis for Lower-Critical Dimension

Below we apply domain-wall arguments to estimate the lower-critical dimension d_l, above which an ordered state should occur in the corresponding nearest-neighbor version of the present model. Our arguments follow closely those used for the random-field Ising model [5, 41], which were confirmed later by means of a rigorous proof in Ref. [42]. In order to carry out such analysis, we rewrite Eq. (4) as

$$\mathcal{H}(\{h_i^\tau, h_i^\sigma\}) = -J \sum_{\langle ij \rangle} \sigma_i \sigma_j - J \sum_{\langle ij \rangle} \tau_i \tau_j - D \sum_{i=1}^{N} \tau_i \sigma_i - \sum_{i=1}^{N} h_i^\tau \tau_i - \sum_{i=1}^{N} h_i^\sigma \sigma_i \ , \qquad (31)$$

where the summations $\sum_{\langle ij \rangle}$ now correspond to distinct nearest-neighbor pairs of spins on a regular lattice of dimension d.

One should remind that the two ferromagnetic phases that appeared in some of the phase diagrams shown herein are characterized by a single order parameter, $m > 0$, where $m = m_\tau = m_\sigma$ ($D > 0$), or $m = m_\tau = -m_\sigma$ ($D < 0$), so that these phases differ only by the values of the corresponding magnetizations, i.e., $\mathbf{F_1}$ (higher values of m) and $\mathbf{F_2}$ (lower values of m). Consequently, the domain-wall analysis, which consists in estimating energy contributions of the terms of Eq. (31), is not able to identify multicritical points, as well as to distinguish between the two ferromagnetic phases; below, we consider such an analysis, which applies to the existence of an ordered state, characterized by $m > 0$, i.e., to both phases $\mathbf{F_1}$ and $\mathbf{F_2}$. Therefore, for testing the stability of such an ordered state, we consider the system defined by the Hamiltonian of Eq. (31) in its ground state, at a sufficiently low temperature, and we flip the sign of the magnetization in a large region R of the lattice, characterized by a typical linear size L. Each term in the Hamiltonian of Eq. (31) will contribute to change the ground-state energy; the ferromagnetic interactions will produce an increase in this energy, due to the creation of the interface,

$$\epsilon_J^\tau \sim J L^{d-1} \ ; \qquad \epsilon_J^\sigma \sim J L^{d-1} \ . \qquad (32)$$

Since the fields are quenched random variables characterized by short-range correlations, the quantities $\sum_{i=1}^{N} h_i^\tau \tau_i$ and $\sum_{i=1}^{N} h_i^\sigma \sigma_i$, for large domains, should approach normally distributed random variables, with typical values of the order $\pm(\overline{h_i^2} L^d)^{1/2} = \pm h_0 L^{d/2}$ (i.e., of the order of the width of the Gaussian distribution). One can choose the region of flipped spins such that these contributions lead to a decrease of the ground-state energy, i.e.,

$$\epsilon_h^\tau \sim -h_0 L^{d/2} \ ; \qquad \epsilon_h^\sigma \sim -h_0 L^{d/2} \ . \qquad (33)$$

Hence, if $D = 0$, these two effects compete with each other, the contributions of Eq. (32) favoring the ordered state, whereas those of Eq. (33) destabilizing the ferromagnetic phase. The change in the ground-state energy, due to the flip in the magnetization of the region R, is estimated as

$$\delta = \epsilon_J^\tau + \epsilon_J^\sigma + \epsilon_h^\tau + \epsilon_h^\sigma \sim 2(JL^{d-1} - h_0 L^{d/2}) \ , \tag{34}$$

which, except for the factor of 2, lead precisely to the same contributions of the Ising ferromagnet in the presence of random field [5, 41]. Hence, for sufficiently large L, the ordered state prevails for $d > 2$, whereas the disordered (paramagnetic) phase dominates for $d < 2$, from which one obtains the lower-critical dimension $d_l = 2$.

The introduction of a coupling D between the two Ising variables will have no effects on the interface, whereas those inside the region R will just affect the correlations between the two Ising systems, i.e., they do not contribute to stabilize (or destabilize) the ordered state. Hence, the parameter D in the Hamiltonian of Eq. (31) should not be associated with the appearance of an ordered phase, but rather to the possible occurrence of multicritical behavior in the nearest-neighbor version of the model. Therefore, one should not expect any changes in the lower-critical dimension $d_l = 2$, due to the coupling between the two Ising variables. However, the corresponding energy contribution will depend on the dimension d, in the sense that it may change according to the state of the system, as discussed next. (i) For $d < 2$, where the paramagnetic state prevails, the contribution $-D\sum_{i=1}^{N} \tau_i\sigma_i$ will behave like those of Eq. (33), yielding $\epsilon_D \sim \pm DL^{d/2}$; (ii) For $d > 2$, where the ordered state appears, this contribution will lead to $\epsilon_D \sim -DL^d$ ($D > 0$), enlarging the ferromagnetic phase, as verified in the phase diagrams presented above.

IV. CONCLUSIONS

We have analyzed a ferromagnetic four-state clock model in the presence of an anisotropy field D and different conditions for random fields. The model was considered in the limit of infinite-range interactions, for which the mean-field approach becomes exact. By using a representation of two Ising variables ($\{\tau_i\}$ and $\{\sigma_i\}$ for each site i),

the model was expressed as two ferromagnetic Ising models, each with its own random field ($\{h_i^\tau\}$ and $\{h_i^\sigma\}$, respectively). Moreover, in this representation, the anisotropy field leads to a coupling between these two variable sets, in such a way that $D > 0$ ($D < 0$) favors parallel (antiparallel) alignment of the two Ising systems. We have shown that if there is no correlation between the random fields $\{h_i^\tau\}$ and $\{h_i^\sigma\}$, the Hamiltonian of the system presents a symmetry $D \to -D$. The random fields $\{h_i^\tau\}$ and $\{h_i^\sigma\}$ were considered as following bimodal probability distributions, in two extreme situations, namely, fully correlated random fields, i.e., $h_i^\tau = h_i^\sigma$ $(\forall i)$, for which we have analyzed both $D > 0$ and $D < 0$ cases, and uncorrelated fields, for which we have studied typical values of $D > 0$.

For fully correlated fields, $h_i^\tau = h_i^\sigma = \pm h_0$, all phase diagrams presented the same qualitative behavior, similar to the one of an Ising ferromagnet in the presence of a bimodal random field: the paramagnetic and ferromagnetic phases are separated by a continuous frontier at high temperatures, followed by a first-order one for lower temperatures, with these two critical lines meeting at a tricritical point. Hence, the coupling D between the two systems does not play an important role, from the qualitative point of view. Quantitatively, the cases $D < 0$ presented ferromagnetic phases that increase significantly for sufficiently large values of $|D|$.

For uncorrelated fields, since the Hamiltonian presents the symmetry $D \to -D$, we have restricted our investigation to $D > 0$ only. This situation has shown a very rich critical behavior by varying D, with the possibility of two ferromagnetic phases, $\mathbf{F_1}$ and $\mathbf{F_2}$, besides the usual disordered phase $\mathbf{P}$, as well as a wide variety of critical points. For sufficiently small values of the coupling D, the phase diagram presents a structure typical of two independent Ising models, being qualitatively similar to the phase diagram of the Ising ferromagnet in the presence of a bimodal random field, characterized by a single ferromagnetic phase. By increasing gradually the coupling between the two Ising systems, the additional ferromagnetic phase emerges, with the two ferromagnetic phases, $\mathbf{F_1}$ (higher values of magnetization) and $\mathbf{F_2}$ (lower values of magnetization), being separated by a first-order critical frontier that terminates at an ordered critical point.

Therefore, in the case of uncorrelated fields we have found five well-defined types of phase diagrams, denominated as topologies I–V, which differ from one another by the presence of distinct critical behavior, with tricritical, fourth-order, ordered, triple,

multicritical, and critical end points. These qualitatively different types of phase diagrams correspond to the intervals $0 < (D/J) \leq 0.3535$ (topology I), $0.3535 < (D/J) \leq 0.470$ (topology II), $0.472 \leq (D/J) < 0.5$ (topology III), $(D/J) = 0.5$ (topology IV), and $(D/J) > 0.5$ (topology V). The change from topologies II and III is very subtle from the numerical point of view, since this occurs through the disappearance of the critical end point, giving rise to to two other critical points, namely, a triple and a tricritical one. We have found that this occurs for $(D/J) = 0.471 \pm 0.001$, in the sense that topology II holds clearly for $(D/J) = 0.470$, whereas topology III applies for $(D/J) = 0.472$. From all these cases, only topology I typifies a well-known phase diagram, qualitatively similar to the Ising ferromagnet in the presence of a bimodal random field [8].

We have carried heuristic domain-wall arguments for estimating the lower critical dimension, above which an ordered state should appear in the corresponding nearest-neighbor version of the model. The study considered an ordered state, characterized by a single magnetization parameter, so that it applies to both phases $\mathbf{F_1}$ and $\mathbf{F_2}$. These arguments led to $d_l = 2$, i.e., the same lower critical dimension of the Ising ferromagnet in the presence of a random field. Our analysis indicated that the coupling D does not contribute to change d_l; however, the gradual increase of D should be associated with a possible occurrence of multicritical behavior, as well as to an enlargement of the ordered phase.

From the physical point of view, the first situation considered herein, namely, fully correlated fields, would correspond to a situation where in each position i the fields $\{h_i^\tau\}$ and $\{h_i^\sigma\}$ are the same, being associated to random effects due to the medium only. The second case, where in each position i one has independent fields $\{h_i^\tau\}$ and $\{h_i^\sigma\}$, may result from randomnesses of the medium, in addition to other possible effects (e.g., from the remaining spin variables), such as to act distinctly on the systems $\{\tau_i\}$ and $\{\sigma_i\}$. However, since the Ising model is well-known to provide a wide applicability in many complex systems so far, the richness of critical behavior exhibited by the model studied herein, with phase diagrams presenting new and interesting topologies, is expected to be useful for other complex phenomena, out of the scope of magnetism.

Acknowledgments

The partial financial support from CNPq, FAPEAM-Projeto-Universal-Amazonas, and FAPERJ (Brazilian funding agencies) is acknowledged.

---

[1] P. M. Chaikin and T. C. Lubensky, *Principles of Condensed Matter Physics* (Cambridge University Press, Cambridge, 1995).

[2] K. Huang, *Statistical Mechanics*, second edition (John Wiley and Sons, New York, 1987).

[3] W. P. Wolf, The Ising Model and Real Magnetic Materials, Braz. J. Phys. **30**, 794 (2000).

[4] A. P. Young, editor, *Spin Glasses and Random Fields* (World Scientific, Singapore, 1998).

[5] V. Dotsenko, *Introduction to the Replica Theory of Disordered Statistical Systems* (Cambridge University Press, Cambridge, 2001).

[6] H. Nishimori, *Statistical Physics of Spin Glasses and Information Processing* (Oxford University Press, Oxford 2001).

[7] T. Schneider and E. Pytte, Random-field instability of the ferromagnetic state, Phys. Rev. B **15**, 1519 (1977).

[8] A. Aharony, Tricritical points in systems with random fields, Phys. Rev. B **18**, 3318 (1978).

[9] D. Andelman, First- and second-order phase transitions with random fields at low temperatures, Phys. Rev. B **27**, 3079 (1983).

[10] S. Galam and J. Birman, Random-field distributions and tricritical points, Phys. Rev. B **28**, 5322 (1983).

[11] D. C. Mattis, Tricritical Point in Random-Field Ising Model, Phys. Rev. Lett. **55**, 3009 (1985).

[12] M. Kaufman, P. E. Kluzinger and A. Khurana, Multicritical points in an Ising random-field model, Phys. Rev. B **34**, 4766 (1986).

[13] A. Benyoussef, T. Biaz, M. Saber and M. Touzani, The spin-1 Ising model with a random crystal field: the mean-field solution, J. Phys. C **20**, 5349 (1987).

[14] M. Kaufman and M. Kanner, Random-field Blume-Capel model: Mean-field theory, Phys. Rev. B **42**, 2378 (1990).

[15] S. Galam, S. R. Salinas and Y. Shapir, Randomly coupled Ising models, Phys. Rev. B **51**, 2864 (1995).

[16] E. Nogueira Jr., F. D. Nobre, F. A. da Costa, and S. Coutinho, Tricritical behavior in the Sherrington-Kirkpatrick spin glass under a bimodal random field, Phys. Rev. E **57**, 5079 (1998); Erratum, Phys. Rev. E **60**, 2429 (1999).

[17] J. M. de Araújo, F. D. Nobre, and F. A. da Costa, Tricritical points in the Sherrington-Kirkpatrick model in the presence of discrete random fields, Phys. Rev. E **61**, 2232 (2000).

[18] N. Crokidakis and F. D. Nobre, Destruction of first-order phase transition in a random-field Ising model, J. Phys. Condens. Matter **20**, 145211 (2008).

[19] N. Crokidakis and F. D. Nobre, Ising spin glass under continuous-distribution random magnetic fields: Tricritical points and instability lines, Phys. Rev. E **77**, 041124 (2008).

[20] O. R. Salmon, N. Crokidakis, and F. D. Nobre, Multicritical behavior in a random-field Ising model under a continuous-field probability distribution, J. Phys.: Condens. Matter **21**, 056005 (2009).

[21] O. R. Salmon and J. Rojas, Multicriticality in the Blume-Capel model under a continuous-field probability distribution, J. Phys. A: Math. Theor. **43**, 125003 (2010).

[22] O. R. Salmon and F. D. Nobre, Multicritical behavior of two coupled Ising models in the presence of a random field, Phys. Rev. E **89**, 062104 (2014).

[23] S. Galam, Plastic Crystals, Melting, and Random Fields, Phys. Lett. A **122**, 271 (1987).

[24] S. Galam and M. Gabay, Coupled Spin Systems and Plastic Crystals, Europhys. Lett. **8**, 167 (1989).

[25] E. Vives and A. Planes, Critical behavior of a system with orientational and positional degrees of freedom: A Monte Carlo simulation study, Phys. Rev. B **43**, 13335 (1991).

[26] R. J. Baxter, *Exactly Solved Models in Statistical Mechanics* (Academic Press, London, 1982).

[27] F. Y. Wu, The Potts Model, Rev. Mod. Phys. **54**, 235 (1982).

[28] S. Fishman and A. Aharony, Random field effects in disordered anisotropic antiferromagnets, J. Phys. C **12** , L729 (1979).

[29] Po-Zen Wong, S. von Molnar, and P. Dimon, Random-field effects in $Fe_{1-x}Mg_xCl_2$, J. Appl. Phys. **53** , 7954 (1982).

[30] J. Cardy, Random-field effects in site-disordered Ising antiferromagnets, Phys. Rev. B **29** , 505 (1984).

[31] R. B. Griffiths, Phase diagrams and higher-order critical points, Phys. Rev. B **12**, 345 (1975).

[32] K. Binder and D. P. Landau, Multicritical Phenomena at Surfaces, Surface Science **61**, 577 (1976).

[33] R. Pynn and A. Skjeltorp, editors, *Multicritical Phenomena* (Plenum Press, New York, 1984).

[34] D. I. Uzunov, *Introduction to the Theory of Critical Phenomena* (World Scientific Publishing Co., Singapore, 1993).

[35] R. Zach, M. Guillot, J. C. Picoche, and R. Fruchart, Critical field behaviour of $MnFeAs_yP_{1-y}$ system, J. Mag. Mag. Mat. **140-144**, 1541 (1995).

[36] B. Lambert-Andront, J. Pierre, B. Chenevier, R. Madar, N. Boutarek, and J. Rodriguez-Carvajal, The coexistence of two phases with ordered and disordered vacancies in $PrGe_{1.6}$, J. Phys.: Condens. Matter **6**, 8725 (1994).

[37] P. Schobinger-Papamantellos, D. B. de Mooij, and K. H. J. Buschow, Modulated structure and ferromagnetic ordering in $PrGe_{1.6}$ studied by neutron diffraction and magnetic measurements, J. Mag. Mag. Mat. **89**, 47 (1990).

[38] J. Kushauer, R. van Bentum, W. Kleemann, and D. Bertrand, Athermal magnetization avalanches and domain states in the site-diluted metamagnet $Fe_xMg_{1-x}Cl_2$, Phys. Rev. B **53**, 11647 (1996).

[39] J. Kushauer and W. Kleemann, Random-field destructed first-order phase transition in $Fe_xMg_{1-x}Cl_2$, J. Mag. Mag. Mat. **140-144**, 1551 (1995).

[40] R. B. Griffiths and B. Widom, Multicomponent-Fluid Tricritical Points, Phys. Rev. A **8**, 2173 (1973).

[41] Y. Imry and S.-K. Ma, Random-Field Instability of the Ordered State of Continuous Symmetry, Phys. Rev. Lett. **35**, 1399 (1975).

[42] J. Imbrie, Lower Critical Dimension of the Random-Field Ising Model, Phys. Rev. Lett.

53, 1747 (1984).